

## Supplementary Materials for

### **Label-free sensing of exosomal MCT1 and CD147 for tracking metabolic reprogramming and malignant progression in glioma**

A. Thakur, G. Qiu, C. Xu, X. Han, T. Yang, S. P. NG, K. W. Y. Chan, C. M. L. Wu\*, Y. Lee\*

\*Corresponding author. Email: [younglee@cityu.edu.hk](mailto:younglee@cityu.edu.hk) (Y.L.); [lawrence.wu@cityu.edu.hk](mailto:lawrence.wu@cityu.edu.hk) (C.M.L.W.)

Published 26 June 2020, *Sci. Adv.* **6**, eaaz6119 (2020)

DOI: [10.1126/sciadv.aaz6119](https://doi.org/10.1126/sciadv.aaz6119)

#### **This PDF file includes:**

Figs. S1 to S10

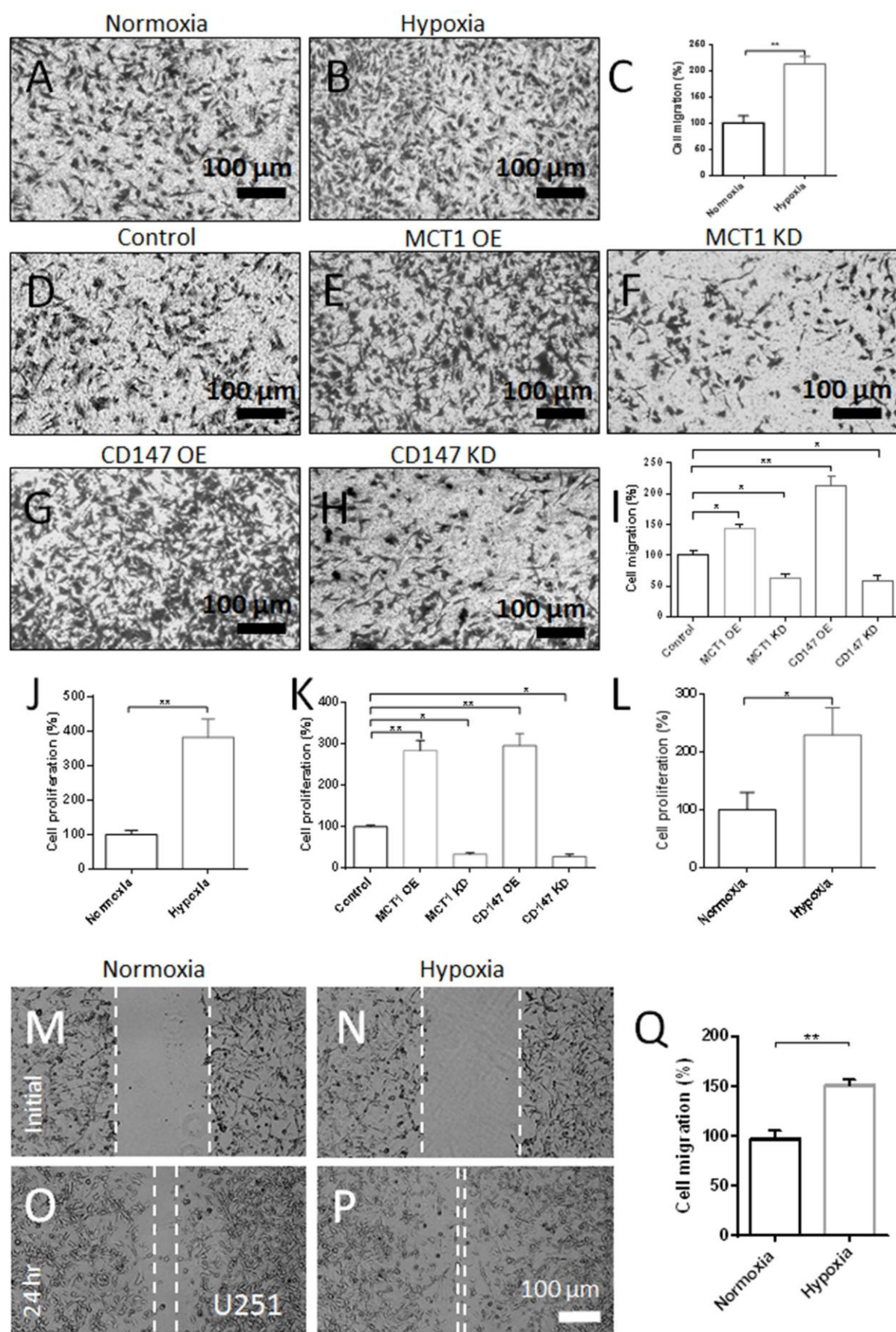


**Fig. S1 MCT1 and its binding partner, CD147, play a crucial role in the hypoxia-induced malignant progression of U251 GMs.** (A-B, D-H) Representative images of GMs' migration under normoxia or hypoxia (1% O<sub>2</sub>) for 24 hours and their migration with the induction of MCT1 OE, MCT1 KD, CD147 OE, or CD147 KD compared to control for 24 hours, as detected by transwell migration assay. (C, I) Quantitative analysis for GMs' migration by counting the number of migrated cells in transwell assay (n=6 with ImageJ software). Relative GMs' migration (%) is expressed as the percent change relative to a respective control (100%). (J, K) Comparative analysis of GMs' proliferation among normoxic and hypoxic GMs as well as MCT1 OE-, MCT1 KD-, CD147 OE-, and CD147 KD- induced GMs, compared to control, using MTT cell proliferation assay (n=6) as described in Methods. (L) BrdU cell proliferation assay for GMs under normoxia or hypoxia (n=6). Relative GMs' proliferation (%) is expressed as the percent change relative to the respective control (100%). (M-P) Enhanced migration of U251 GMs under hypoxia for 24 hours as detected by scratch assay. (Q) Quantitative analysis for U251 GMs' migration by ImageJ software (n=6). Relative migration (%) was expressed as the percent change relative to a respective control (100%). Data shown here are presented as the mean ± standard deviation (SD) of 2 independent experiments. Significance level: \*\* P < 0.01, \*P < 0.05, hypoxia vs. normoxia. MCT1 OE-, MCT1 KD-, CD147 OE-, or CD147 KD- group vs. control. Scale bar in A-B and D-H: 100 μm.

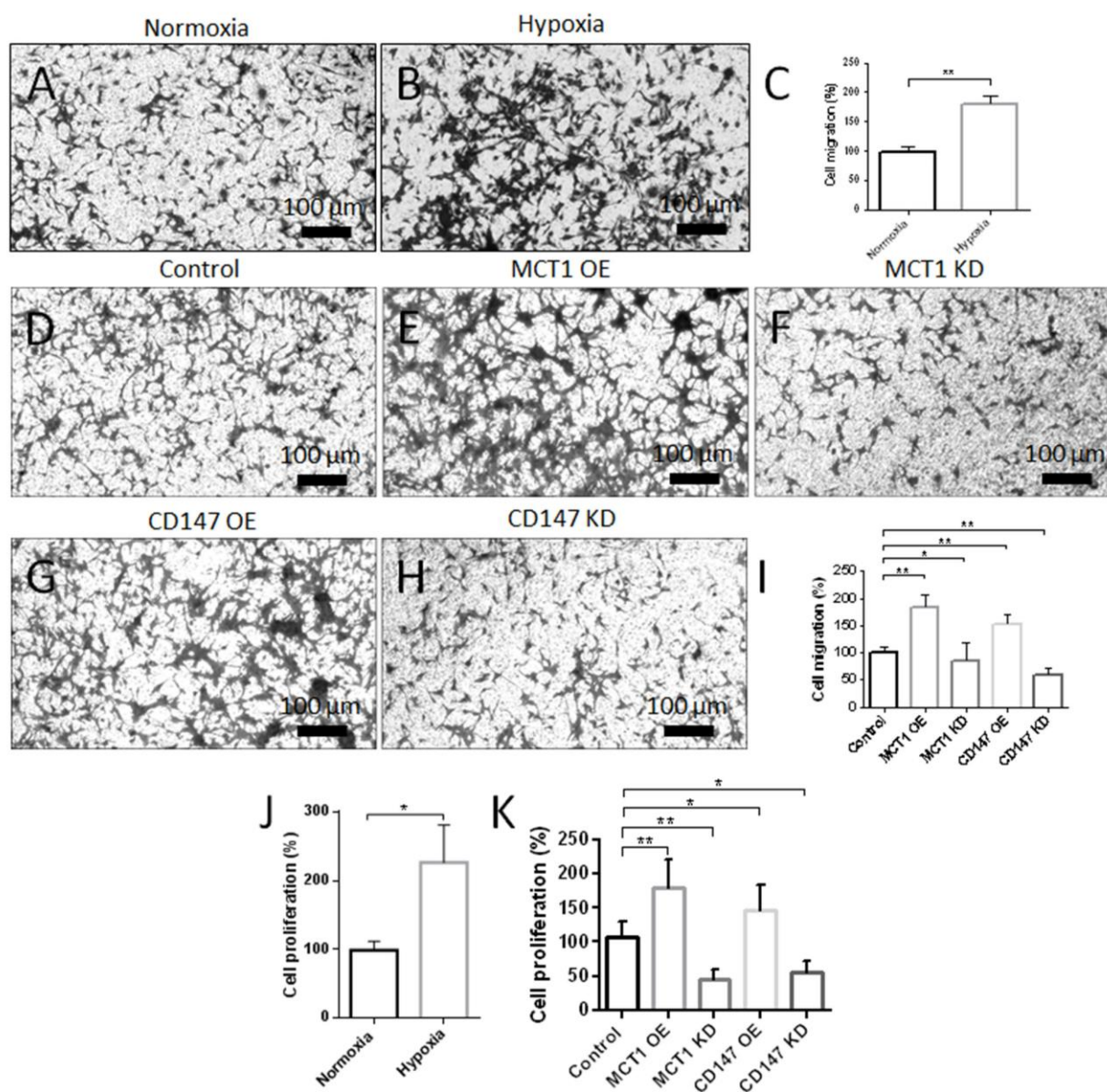


**Fig. S2.** (A-B and D-H) Representative images of U87 GMs' migration under normoxia or hypoxia (1% O<sub>2</sub> in a modular chamber) for 24 hours and their migration in response to MCT1 OE, MCT1 KD, CD147 OE, or CD147 KD compared to untreated control for 24 hours as detected by transwell migration assay. (C and I) Quantitative analysis for U87 GMs' migration by counting the number of migrated cells in six different fields with ImageJ software (n=6). Relative migration (%) was expressed as the percent change relative to a respective control (100%). (J-K) Comparative analysis of U87 GMs' proliferation among normoxic-, hypoxic-, MCT1 KD-, or CD147 KD- group compared to untreated control using MTT cell proliferation assay (n=6), as described in Methods. Relative proliferation (%) was expressed as the percent change relative to a respective control (100%). Results were presented as the mean  $\pm$  SD of 2 independent experiments, each performed in 1 time. Significance level: \*\*  $P < 0.01$ , \*  $P < 0.05$ , hypoxia vs. normoxia. MCT1 OE-, MCT1 KD-, CD147 OE-, or CD147 KD- group vs. control. Scale bar in A-B and D-H: 100  $\mu$ m.

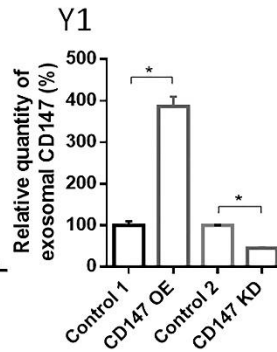
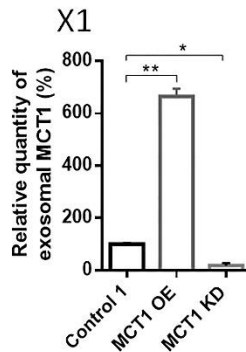
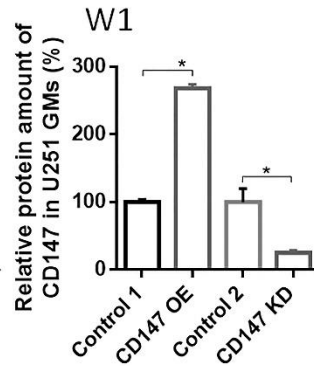
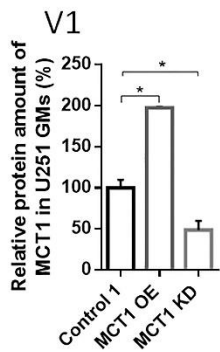
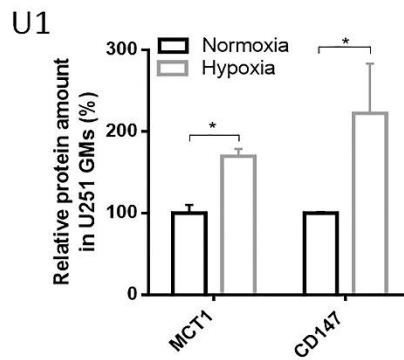
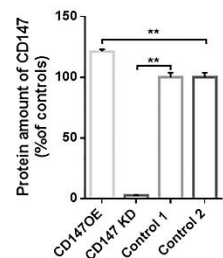
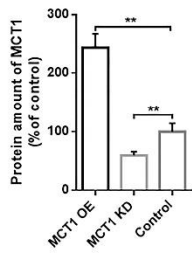
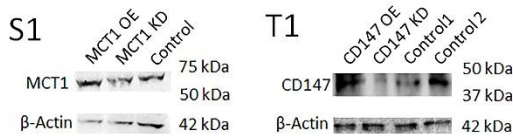
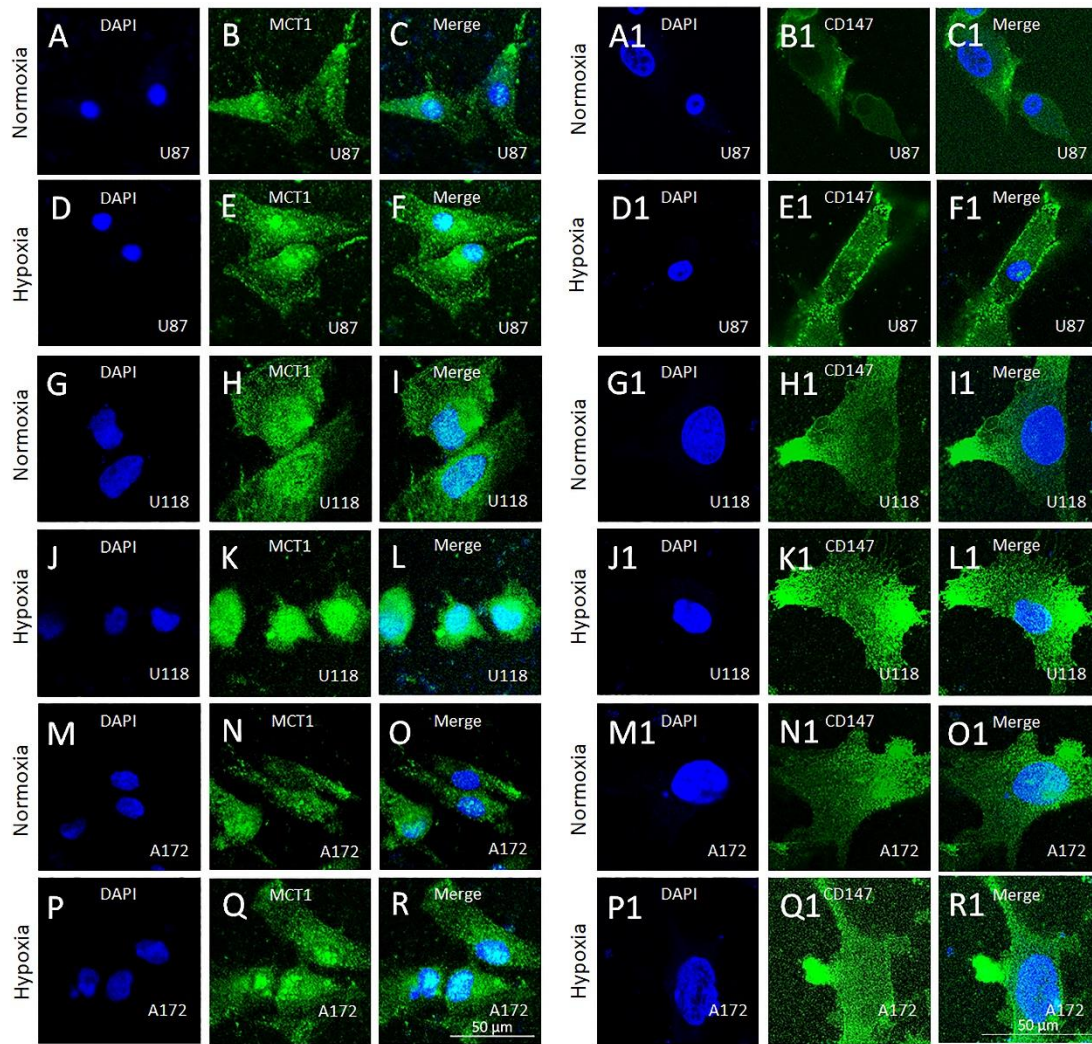
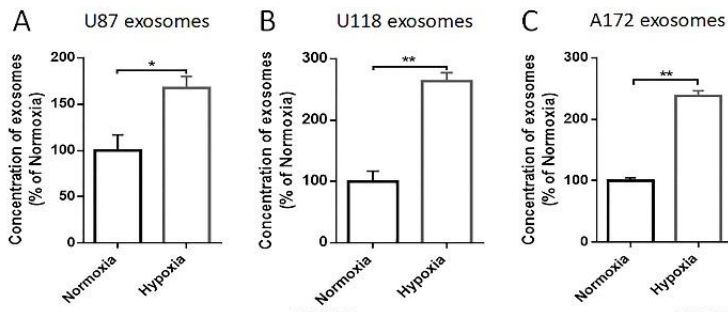


**Fig. S3. MCT1 and CD147 expression in various glioma cell lines under normoxia or hypoxia, determination of the efficacy of MCT1- and CD147- KD and OE in GMs, and determination of MCT1 and CD147 levels in GMs and GMs-derived exosomes by ELISA.** (A-R) Immunofluorescent staining of MCT1 in U87 GMs (A-F), U118 GMs (G-L), and A172 GMs (M-R) under normoxia or hypoxia (1% oxygen). (A1-R1) Immunofluorescent staining of CD147 in U87 GMs (A1-F1), U118 GMs (G1-L1), and A172 GMs (M1-R1) under normoxia or hypoxia (1% oxygen). Scale bar in A-R and A1-R1: 50  $\mu$ m. Nucleus: DAPI (blue), MCT1 and CD147: Alexa 488 (green). (S1) MCT1 level in U251 GMs with treatment of MCT1 OE-, MCT1 KD-, or empty backbone- lentivirus (control) for 24 hours, as determined by WB. (T1) CD147 level in U251 GMs with treatment of CD147 OE, control 1 (lentivirus control), CD147 KD (antisense LNA GapmeR), or control 2 (antisense control) for 24 hours, as determined by WB. (U1) Relative MCT1 and CD147 levels in U251 GMs under normoxia and hypoxia, as detected by ELISA. (V1, W1) Relative MCT1 and CD147 levels in the U251 GMs with the induction of MCT1 OE, MCT1 KD, CD147 OE, CD147 KD, and respective controls, as detected by ELISA. (X1, Y1) Relative MCT1 and CD147 levels in the exosomes derived from the U251 GMs with the induction of MCT1 OE, MCT1 KD, CD147 OE, CD147 KD, and respective controls, as detected by ELISA. All data were expressed as the mean  $\pm$  SD. Significance level: \*\*  $P < 0.01$ , \* $P < 0.05$ , hypoxia vs. normoxia, MCT1 OE or MCT1 KD group vs. control 1, CD147 OE and CD147 KD group vs. control 1 and 2, respectively.



U87 Exosomes      U118 Exosomes      A172 Exosomes

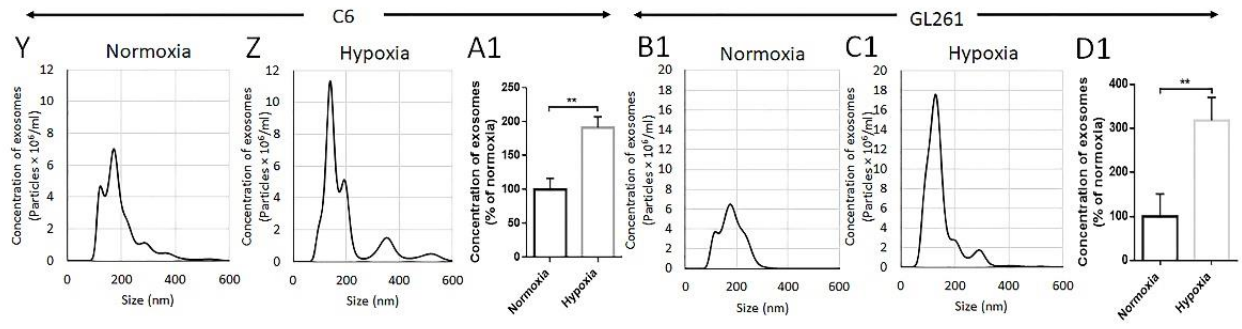
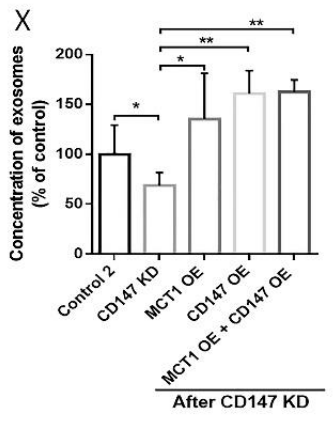
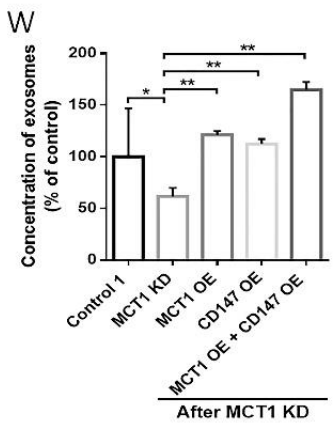
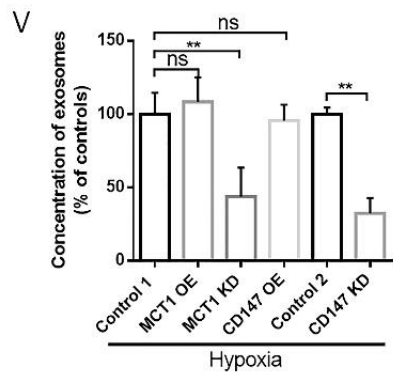
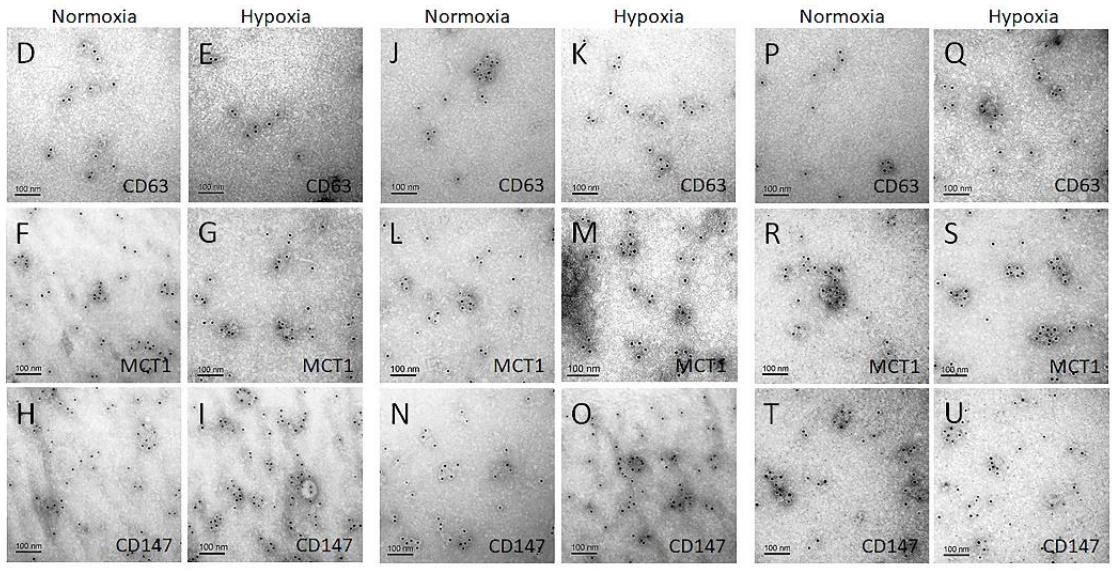


**Fig. S4 Detection of exosome release and exosomal CD63, MCT1, and CD147 from normoxic and hypoxic GMs.** Exosome release is enhanced from (A) U87 GMs, (B) U118 GMs, and (C) A172 GMs under hypoxia compared to normoxia, as detected by NTA (n=9). Representative immunogold EM micrographs for CD 63, MCT1, and CD147 in exosomes derived from normoxic and hypoxic (D-I) U87 GMs, (J-O) U118 GMs, and (P-U) A172 GMs. Scale bar = 100 nm. (V) Effect of MCT1 OE, MCT1 KD, CD147 OE, and CD147 KD on the exosome release from U251 GMs under hypoxia. (W, X) Effect MCT1 OE, CD147 OE, simultaneous OE of MCT1 and C147, after MCT1 KD or CD147 KD in GMs. Enhanced release of exosomes from (Y, Z, A1) hypoxic C6 GMs, and (B1, C1, D1) hypoxic GL261 GMs compared to normoxia. All data were expressed as the mean  $\pm$  SD. Significance level: \*\* P < 0.01, \*P < 0.05, hypoxia vs. normoxia. MCT1 OE-, MCT1 KD-, CD147 OE group vs. control 1. CD147 KD- group vs. control 2.



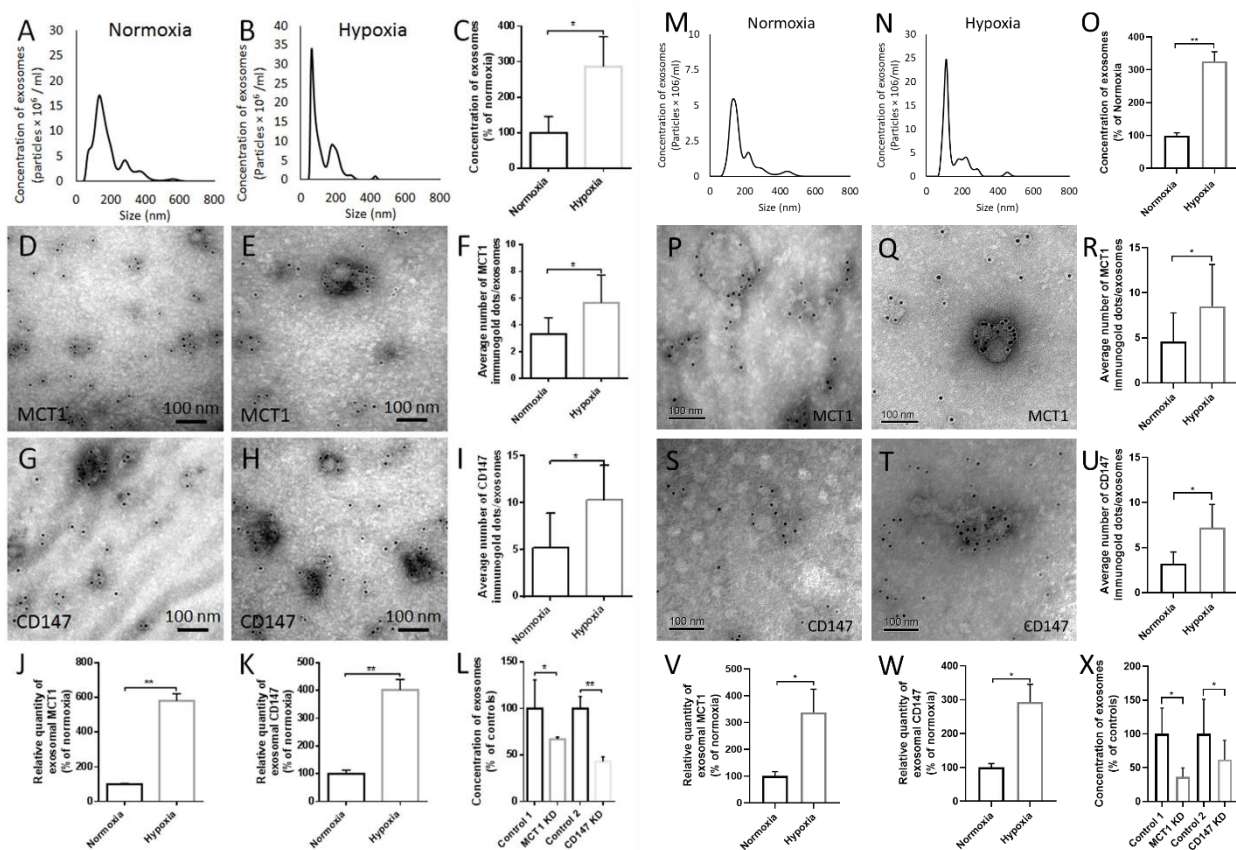


**Fig. S5 Detection of exosome release and exosomal MCT1 and CD147 from normoxic and hypoxic glioma stem cells (GSCs).** Representative size distribution of exosomes from (A) normoxic- and (B) hypoxic- SF7761 GSCs. Exosome release is enhanced from (C) SF7761 GSC under hypoxia compared to normoxia, as detected by NTA (n=9). Representative immunogold dots and their quantification for (D-F) MCT1, and (G-I) CD147 in exosomes derived from normoxic- and hypoxic- SF7761 GSCs. Scale bar = 100 nm. (J, K) Bar graphs showing the relative quantity of MCT1 and CD147 in exosomes from normoxic and hypoxic SF7761 GSCs as detected by ELISA. (L) Effect of MCT1 KD or CD147 KD on exosome release from SF7761 GSCs compared to control 1 (empty backbone- lentivirus) or control 2 (antisense oligonucleotides control) respectively. Representative size distribution of exosomes from (M) normoxic- and (N) hypoxic- SF7761 GSCs. Exosome release is enhanced from (O) human GBM CSCs (Cat# 36104-41, Celprogen) under hypoxia compared to normoxia, as detected by NTA (n=9). Representative immunogold dots and their quantification for (P-R) MCT1, and (S-U) CD147 in exosomes derived from normoxic- and hypoxic- SF7761 GSCs. Scale bar = 100 nm. (V, W) Bar graphs showing the relative quantity of MCT1 and CD147 in exosomes from normoxic and hypoxic human GBM CSCs as detected by ELISA. (X) Effect of MCT1 KD or CD147 KD on exosome release from SF7761 GSCs compared to control 1 (empty backbone- lentivirus) or control 2 (antisense oligonucleotides control) respectively. All data were expressed as the mean  $\pm$  SD. Significance level: \*\*  $P < 0.01$ , \* $P < 0.05$ , hypoxia vs. normoxia, MCT1 KD vs. control 1, CD147 KD vs. control 2.

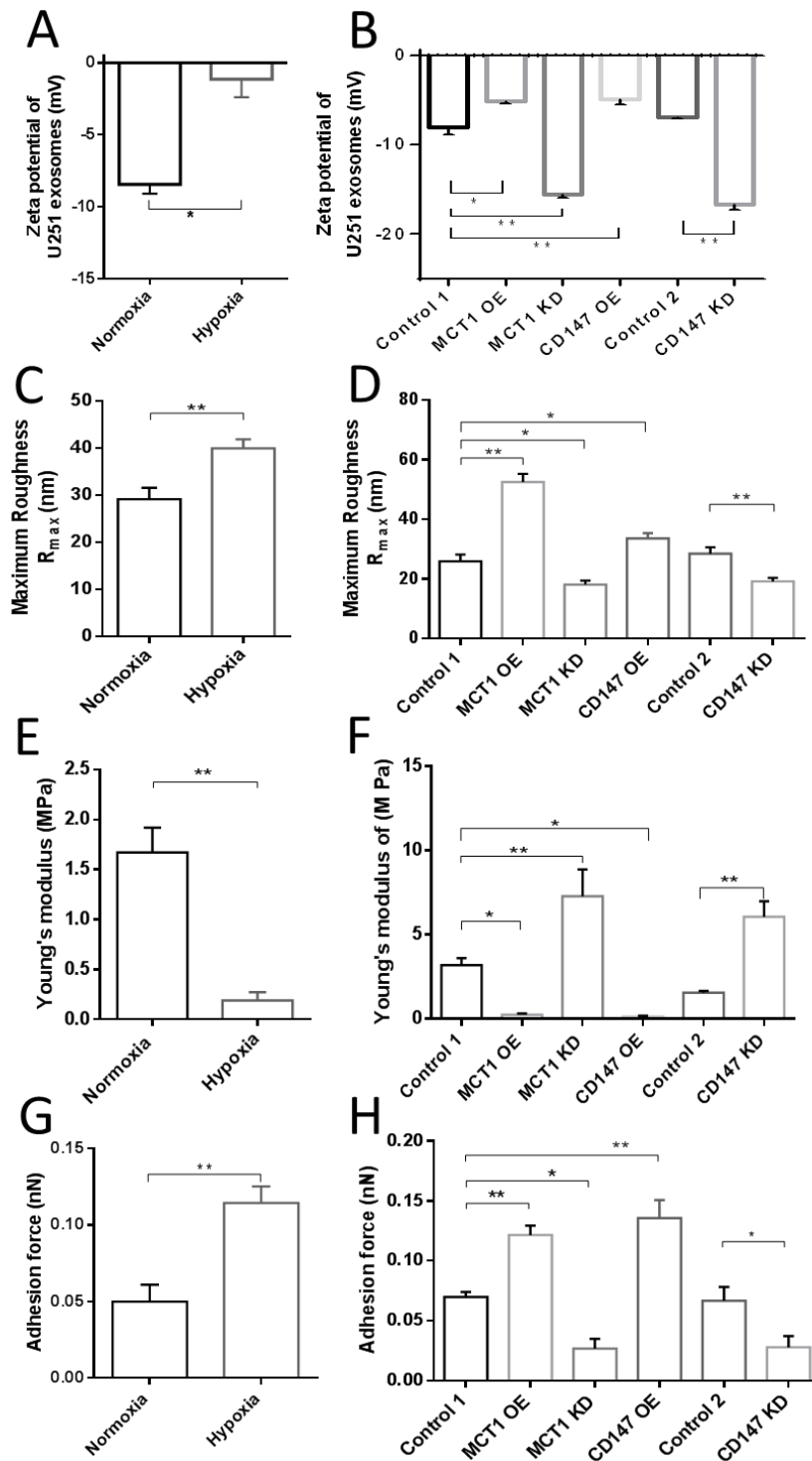


**Fig. S6 Effect of MCT1 OE and MCT1 KD on the biophysical properties of exosomes derived from U251 GMs.** (A-B) Zeta potential, (C-D) Roughness, (E-F) Stiffness (Young's modulus), and (G-H) Adhesion force of exosomes derived from normoxic and hypoxic U251 GMs as well as U251 GMs with the induction of MCT1 OE, MCT1 KD, CD147 OE, and CD147 KD (as compared to a relevant control: control 1 for lentivirus; control 2 for antisense oligonucleotide). All data were expressed as the mean  $\pm$  SD (N=4), Significance level: \*\*  $P < 0.01$ , \*  $P < 0.05$ , hypoxia vs. normoxia, MCT1 OE-, MCT1 KD-, or CD147 OE- group vs. control 1. CD147 KD group vs. control 2.

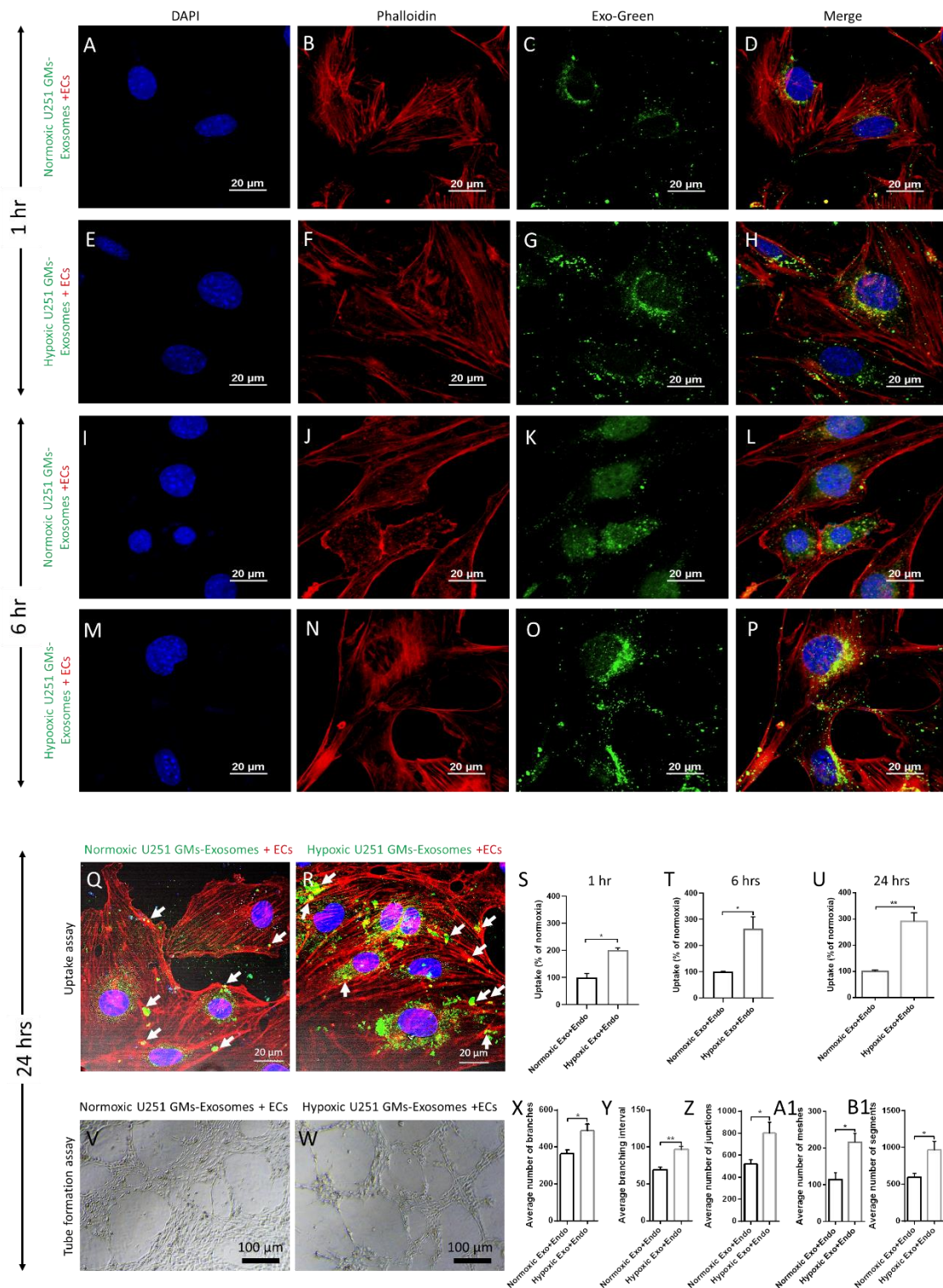


**Fig. S7 Effect of hypoxic GMs- derived exosomes on their uptake into ECs and angiogenesis.** Uptake of (A-D, I-L, Q, S-U) normoxic and (E-H, M-P, Q, S-U) hypoxic U251 GMs- derived exosomes by bEnd3 ECs at 1 hr., 6 hrs., and 24 hrs. Blue: DAPI, Red: Phalloidin, Green: Exo-Green (hypoxic or normoxic U251 GMs-derived exosomes). Representative images for tube formation of bEnd3 ECs, as an angiogenesis assay, by the uptake of (V, W) normoxic and hypoxic U251 GMs- derived exosomes. (X-Z, A1, B1) Bar graphs represent enhanced number of branches, branching interval, junctions, meshes, and segments in ECs treated with hypoxic GMs-exosomes compared to the normoxic GMs-exosomes. All data were expressed as the mean  $\pm$  SD. Significance level: \*\*  $P < 0.01$ , \*  $P < 0.05$ , hypoxia vs. normoxia.

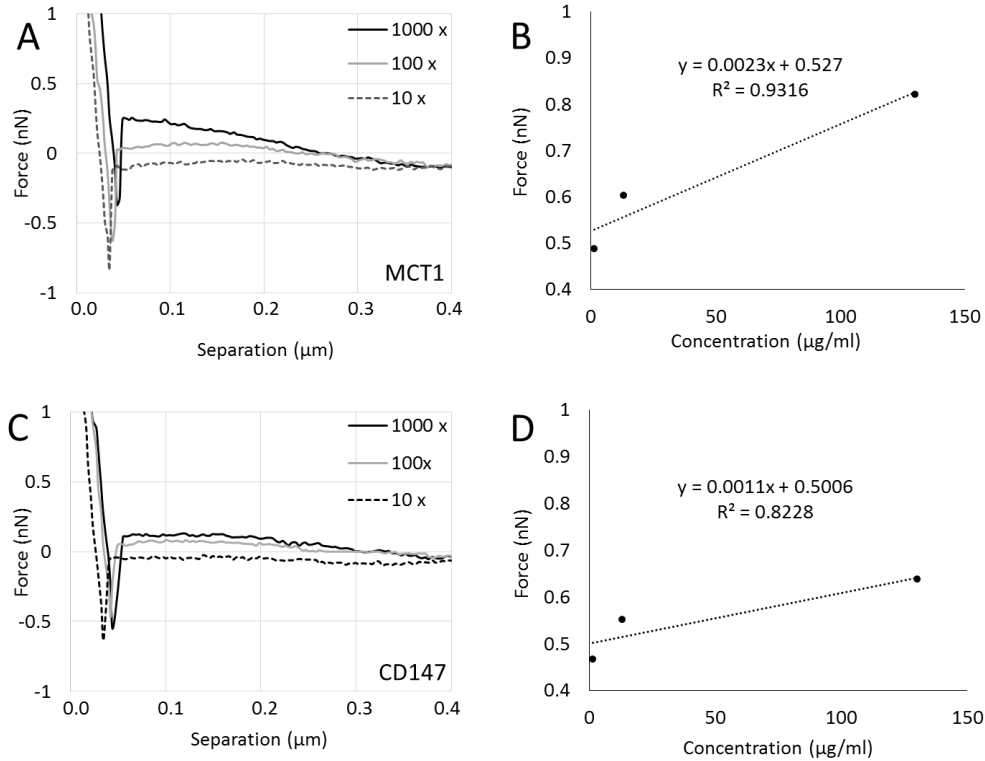


**Fig. S8 Detection sensitivity of AFM having the functionalized tip with anti-MCT1 AB, or anti-CD147 AB toward exosomes.** (A, C) AFM separation curves between the functionalized sensing tip with anti-MCT1 AB, or anti-CD147 AB toward exosomes on the SAM-AuNIs sample discs, which were captured by anti-CD63AB, from three different concentrations of initial exosome solutions (Serial dilution: 1000x, 100x, and 10x of 500  $\mu\text{g/ml}$  protein concentration) from U251 GM. (B, D) Correlation curve between exosome concentration and the strength of AFM forces toward exosomal MCT1 or CD147, respectively (for MCT1;  $R^2=0.9316$  and for CD147;  $R^2=0.8228$ ).

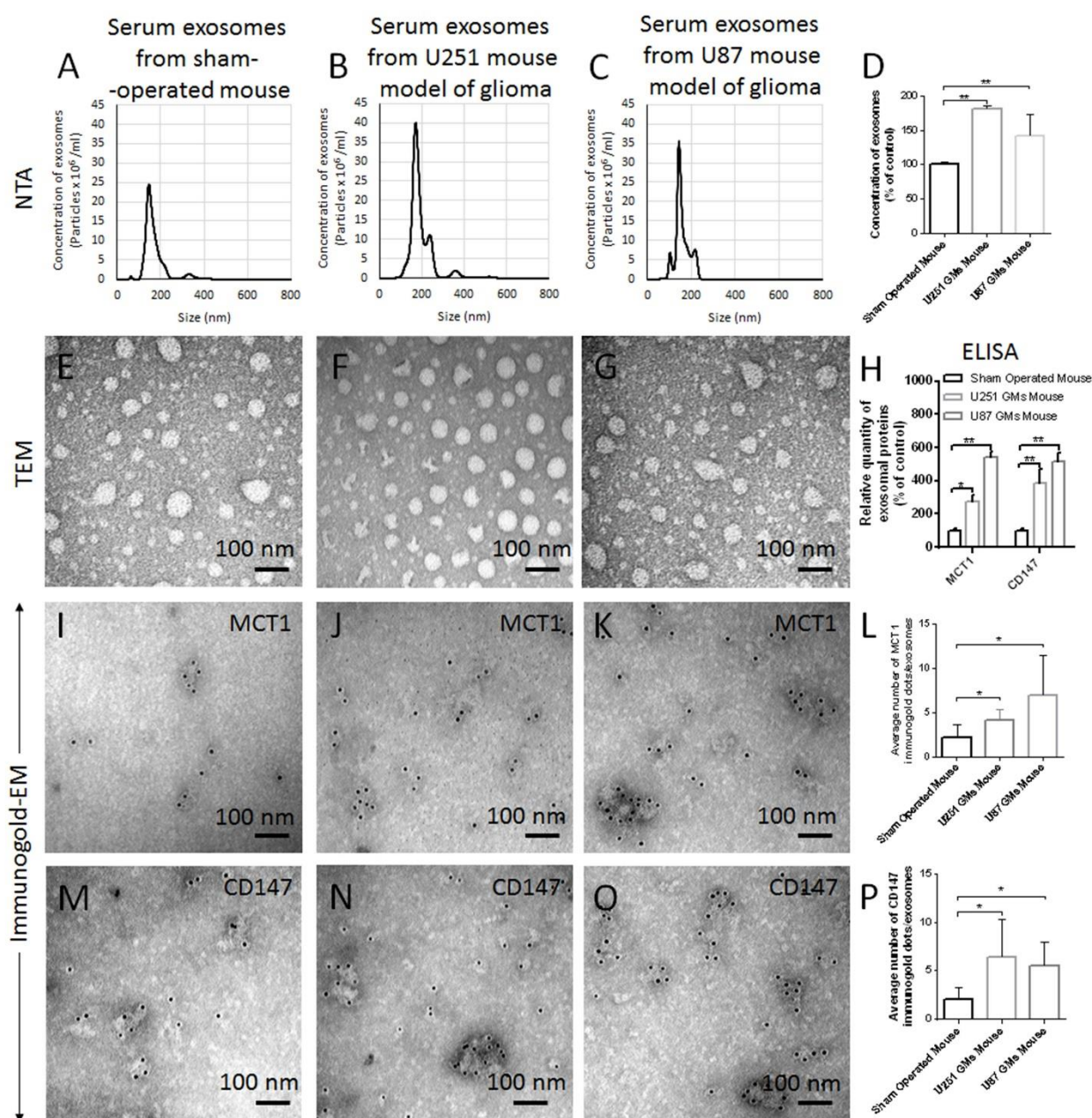


**Fig. S9 Detection of exosome release and exosomal MCT1 and CD147 from blood serum of sham-operated mice, U251- and U87- mouse models of glioma.** (A-D) Size distribution and release quantity of exosomes from sham-operated mice (control), and the U251- and U87- glioma model of mice that was detected by NTA. (E-G) Morphology of exosomes-, (H) relative protein amount of MCT1 and CD147-, (I-L) positive gold dots for MCT1 and (M-P) CD147 in exosomes- from sham-operated mice (control), and U251- and U87- glioma mouse model, as detected by TEM and immunogold EM, respectively. All data were expressed as the mean  $\pm$  SD. Significance level: \*\*  $P < 0.01$ , \*  $P < 0.05$ , U251- or U87- mouse model of glioma vs. sham-operated mouse.

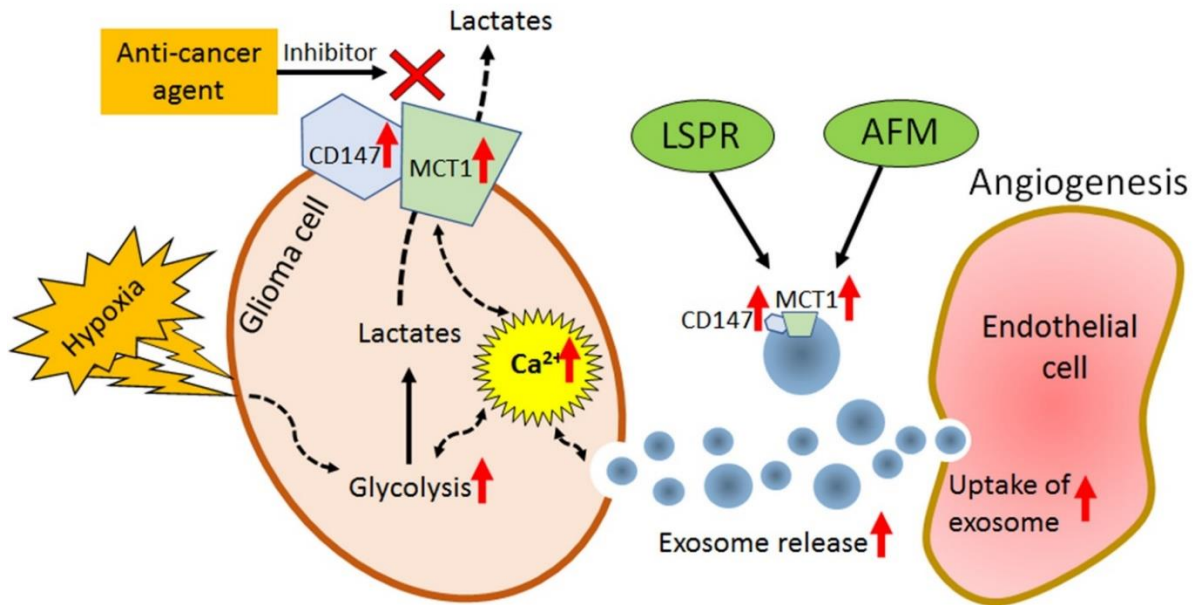


**Fig. S10 Proposed hypothesis for label-free sensing of exosomal MCT1 and CD147 as novel surrogate biomarkers for metabolic reprogramming and malignant progression of glioma.** Under hypoxia, one of the major hallmarks of the tumor microenvironment, the expression of MCT1 and CD147 in GMs are upregulated along with other glycolytic genes to facilitate the exocytosis of increased intracellular lactate. The release of exosomes is enhanced from GMs, which is controlled by MCT1 and CD147 in a calcium-dependent manner. The enhanced exosomal MCT1 and CD147 can be precisely detected by label free SAM-AuNIs LSPR and SAM-AuNIs AFM biosensors to monitor the metabolic reprogramming and malignant progression of glioma.